

# Silicon Nitride Band Splitter Based on Multimode Bragg Gratings

Jonathan Cauchon<sup>1</sup>, Jonathan St-Yves<sup>1</sup>, Francois Menard<sup>2</sup>, and Wei Shi<sup>1\*</sup>

<sup>1</sup> Centre d'optique, photonique et laser (COPL), Université Laval, 2375 rue de la Terrasse, Québec, QC, Canada, G1V 0A6.

<sup>2</sup> AEAPONYX, 33 Prince St., #200A, Montreal (QC), Canada, H3C 2M7.

\* wei.shi@gel.ulaval.ca

**Abstract:** We demonstrate a silicon nitride multimode Bragg grating as a C/L diplexer for single-fiber bidirectional communications. The device was fabricated using optical lithography and achieved a channel isolation greater than 20 dB. © 2021 The Author(s)

**OCIS codes:** (130.3120) Integrated optics devices, (130.7408) Wavelength filtering devices, (350.2770) Gratings, (230.1480) Bragg reflectors.

## 1. Introduction

The pressure of continuously increased Internet data traffic on optical networks leaves service providers with no choice but to adapt their hardware with orders-of-magnitude performance improvements. Next-Generation Passive Optical Network 2 (NG-PON2) is a network architecture utilizing dense wavelength-division multiplexing (DWDM) to achieve higher data rates. Single-fiber NG-PON2 transceivers require a diplexing filter to implement bidirectional communications using C-band channels for upstream transmission and L-band channels for downstream transmission. To meet the NG-PON2 standard and have it coexist with other communication schemes, a high-performance C/L band splitter or diplexing filter implemented in an integrated photonics circuit would be advantageous over currently-used thin film filter (TFF) diplexers requiring free-space integration with lenses.

Among various options for integrated photonic platforms, silicon nitride (Si<sub>3</sub>N<sub>4</sub>) is well known for its low propagation losses, wide transparency spectral range, and compatibility to CMOS processes [1]. A handful of Si<sub>3</sub>N<sub>4</sub>-based broadband filtering devices have emerged over the years. While angled multimode interferometers (angled MMIs) have been envisioned for diplexing filtering [2], they remain to be demonstrated as suitable for filtering on DWDM signals with a sharp roll-off. Arrayed waveguide grating (AWGs) have also been demonstrated on the Si<sub>3</sub>N<sub>4</sub> platform [3] but require considerable on-chip real estate and are not suited for broadband filtering. Conversely, Bragg-based devices offer low-loss, compact and flat-top broadband filtering suitable for C-L band splitting, provided that they can be micro-fabricated using conventional UV lithography in order to be cost effective.

In this work, we propose and experimentally demonstrate, for the first time, a silicon nitride-on-silica multimode Bragg grating (MMBG) filter to isolate the C-band transmission channels (195.3 - 195.6 THz) from the L-band reception channels (187.5 - 187.8 THz). The MMBG is designed anti-symmetrically, so as to allow for efficient coupling between the fundamental and the first higher-order optical modes, resulting in a reflection band in the L-band channels region. While the sidewall-corrugation-enabled grating allows for broadband flat-top filtering, an adiabatic directional coupler (ADC) placed on both ends of the MMBG is used as a mode converter to provide low-loss add-drop operation. The device was fabricated using a wafer-scale process with stepper lithography, showing great potential for fully-integrated NG-PON2 applications.

## 2. Design

The proposed device is based on a silicon nitride-on-silica multimode Bragg grating, supporting the fundamental transverse electric (TE) mode TE<sub>0</sub> and the first higher-order TE<sub>1</sub> mode. The waveguide grating is placed between two ADCs as shown in Fig. 1(a). The MMBG's working principle is based on coupled-mode theory (CMT), which predicts that the periodic dielectric perturbation of a waveguide gives rise to coupling between two given modes with field distributions  $\phi_m$  and  $\phi_n$ . CMT predicts a coupling coefficient given by the following overlap integral [4]:

$$\kappa_{mn} = \frac{\omega}{4} \iint \phi_m^*(x,y) \Delta\epsilon(x,y) \phi_n(x,y) dydx, \quad (1)$$

where  $\Delta\epsilon(x,y)$  is the first-order Fourier series approximation of the periodic perturbation imposed upon the waveguide (the corrugations). Equation 1 indicates what optical modes are allowed to be self- or inter-coupled. When

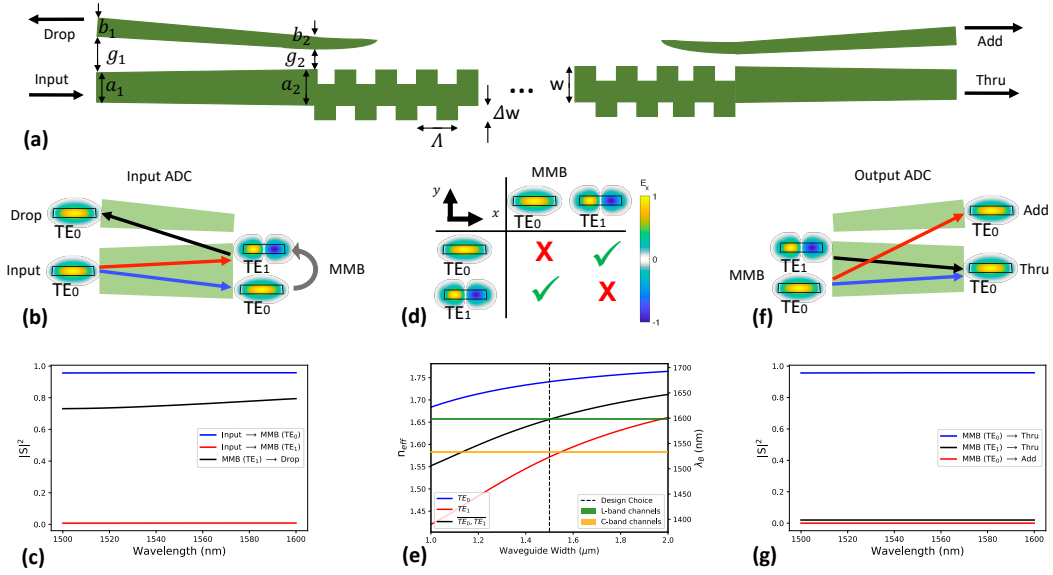


Fig. 1. Design and simulation of the C-L band splitter filter. (a) Scheme of the proposed design, showing the input adiabatic directional coupler (ADC), the multimode Bragg grating, and the output ADC along with all their dimension symbols. (b-c) Scheme and simulated power transmission spectra of the input ADC, where the input TE<sub>0</sub> mode is converted to TE<sub>0</sub> and TE<sub>1</sub>, TE<sub>0</sub> is converted to TE<sub>1</sub> by the MMBG, and the backward-fed TE<sub>1</sub> mode is converted to the TE<sub>0</sub> mode in the drop port. (d) TE mode profiles and coupling possibilities following Eq. 1 inside the MMBG. (e) Phase matching condition inside the MMBG as a function of the waveguide width. (f-g) Scheme and simulated power transmission spectra of the output ADC, where most of the power coming from the MMBG is transmitted to the TE<sub>0</sub> mode in the thru port.

the integrand of Eq. 1 is symmetric (or even), the integral results in a non-zero value, and hence possible mode coupling. However, when the integrand is antisymmetric (or odd), it integrates to a null value and no coupling is undergone. As shown in Fig. 1(a), we use an antisymmetric Bragg grating in our design. Accordingly, the  $\Delta\epsilon(x, y)$  coefficient in Eq. 1 is antisymmetric, and the product only integrates to a non-zero value for the coupling between a symmetric and an antisymmetric mode. In our case, the forward TE<sub>0</sub> mode couples with the backward TE<sub>1</sub> mode, and *vice versa*. The self-coupling of any individual mode is however prohibited. Fig. 1(d) shows the considered modes' spatial distributions and a summary of the coupling possibilities.

Bragg's Law predicts a phase-matching condition given by  $\beta_m + \beta_n = 2\pi/\Lambda$ , where  $\beta = 2\pi n_{eff}/\lambda$  is the propagation constant (with the propagation direction accounted for) and  $\Lambda$  the grating pitch. When inter-modal coupling occurs, the Bragg reflection is located at  $\lambda_B = 2\Lambda n_{eff}$ . That is, the reflection occurs at the average reflection wavelengths of each individual mode [5]. Figure 1(e) shows the simulated effective indices and Bragg wavelengths based on a 484-nm pitch  $\Lambda$  for all supported modes as well as their average value as a function of the waveguide width. A waveguide width  $w$  of 1.5  $\mu\text{m}$  was consequently chosen to allow a reflection at 1600 nm (centered around the reception channels). A corrugation size  $\Delta w$  of 300 nm was chosen to offer broadband filtering. The corrugation size was apodized in a Gaussian shape along the device in order to avoid side-lobes in the spectral response, .

To provide circulator-free add-drop operation, ADCs are used on both sides of the MMBG, acting as mode converters. Such ADCs were designed in an asymmetric directional coupler structure linearly tapered in waveguide width ( $a$  and  $b$ ) and coupler gap ( $g$ ), as shown in Fig. 1(a). Following parameters were chosen in our design:  $a_1 = 800$  nm,  $a_2 = 1500$  nm,  $b_1 = 600$  nm,  $b_2 = 400$  nm,  $g_1 = 750$  nm,  $g_2 = 500$  nm, and a total ADC length of 70  $\mu\text{m}$ . Figures 1(b-c) and 1(f-g) show the simulated performance, which exhibits an approximately 75% (-1.25 dB) efficiency during the backward mode conversion (from TE<sub>1</sub> to the drop port in Fig. 1(c)). All other transmission spectra exhibit very low simulated losses.

### 3. Experiment and Results

The device was fabricated by AEPOYX on SiN-on-silica wafers with a 450-nm-thick silicon nitride (SiN) thin film (refractive index: 2.05) on a SiO<sub>2</sub> bottom clad. The SiN layer was patterned and etched to form the waveguides and Bragg gratings, using conventional UV lithography in combination with sub-resolution assisted features (SRAFs) to attain the critical dimensions required by Bragg gratings, followed by a SiO<sub>2</sub> top clad.

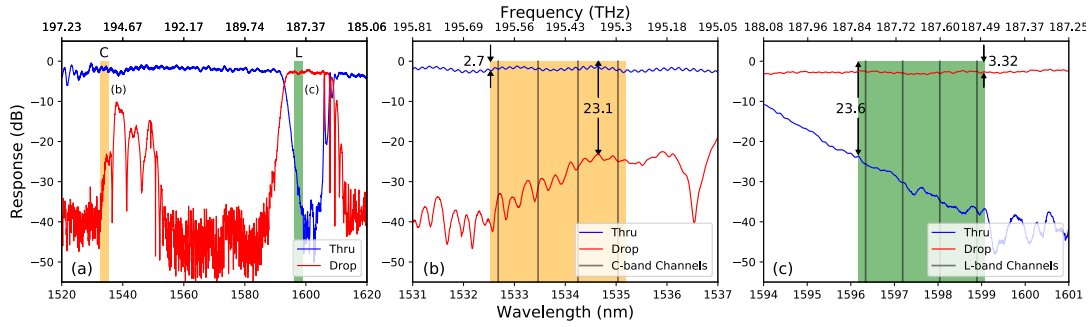


Fig. 2. Measured performance of the filter, showing (a) the overall drop and thru responses with the C- and L-band channels identified, (b) zoomed view of the response at the C-band channels, and (c) zoomed view at the L-band channels.

The fabricated device was tested via surface grating couplers for fiber-to-chip coupling. Fig. 2 shows the filter's measured thru- and drop-port responses, where the L-band channels of interest are dropped, and the C-band channels of interest pass through the filter. The drop response is centered at 1599.6 nm (187.42 THz) and has a 3-dB bandwidth of 12.8 nm (1500 GHz). The C-band channels suffer from an insertion loss of 2.7 dB in the thru-port, while showing an extinction ratio of 20.4 dB at the drop port. Similarly, the target L-band channels show a drop-port insertion loss of 3.32 dB and an extinction ratio of 20.3 dB in the thru port. While both channel bands show similar extinction ratios, the drop-port has an insertion loss slightly higher than the thru port by 0.62 dB. This behavior agrees well with simulation, as observed in Fig. 1(c) that shows that the drop-port mode conversion brings about additional optical loss.

Figure 2 shows the presence of a parasitic reflection band near 1540 nm. Further analysis and simulation has revealed that this parasitic band is caused by the presence of a transverse magnetic- (TM-) polarized optical field component inside the MMBG. That is, the reflection band occurs at the TM mode's phase matching condition. This is attributed to polarization crosstalk in the input ADC. Although it does not impact the drop-port extinction ratio substantially, it can be avoided by further optimization of the adiabatic directional coupler, taking both polarization states into consideration. Moreover, blue shifting the device's reflection spectrum by fine tuning the grating pitch can further improve the overall system performance because the thru-port stop-band will be perfectly aligned with the L-band channels.

#### 4. Conclusion

We have demonstrated a silicon nitride diplexer suitable for single-fiber bidirectional communication applications, achieving a channel isolation greater than 20 dB and a maximum insertion loss of 3.32 dB. Significantly improved performance (higher extinction ratio and lower insertion loss) can be achieved via design optimization of the ADC and MMBG. The fact that the device was implemented using a large-wafer process with UV lithography indicates great potential for mass production.

#### Acknowledgment

This project is supported by the Natural Sciences and Engineering Research Council of Canada (CRDPJ 523096-17), Prompt Québec and AEPONYX inc.

#### References

1. Daniel J Blumenthal, Rene Heideman, Douwe Geuzebroek, Arne Leinse, and Chris Roeloffzen. Silicon nitride in silicon photonics. *Proceedings of the IEEE*, 106(12):2209–2231, 2018.
2. Yaocheng Shi, Jingye Chen, and Hongnan Xu. Silicon-based on-chip diplexing/triplexing technologies and devices. *Science China Information Sciences*, 61(8):080402, 2018.
3. Qi Han, Jonathan St-Yves, Yuxuan Chen, Michaël Ménard, and Wei Shi. Polarization-insensitive silicon nitride arrayed waveguide grating. *Optics letters*, 44(16):3976–3979, 2019.
4. Amnon Yariv and Poçji Yeh. *Photonics: optical electronics in modern communications*. Oxford Univ., 2006.
5. Toru Mizunami, Tzvetanka V Djambova, Tsutomu Niiho, and Sanjay Gupta. Bragg gratings in multimode and few-mode optical fibers. *Journal of lightwave technology*, 18(2):230–235, 2000.